

## Letter to the Editor

# The broad-band (0.1-200 keV) spectrum of Her X-1 observed with *BeppoSAX*

D. Dal Fiume<sup>1</sup>, M. Orlandini<sup>1</sup>, G. Cusumano<sup>2</sup>, S. Del Sordo<sup>2</sup>, M. Feroci<sup>3</sup>, F. Frontera<sup>1,4</sup>, T. Oosterbroek<sup>5</sup>, E. Palazzi<sup>1</sup>, A.N. Parmar<sup>5</sup>, A. Santangelo<sup>2</sup>, and A. Segreto<sup>2</sup>

<sup>1</sup> Istituto Tecnologie e Studio delle Radiazioni Extraterrestri (TeSRE), C.N.R., via Gobetti 101, I-40129 Bologna, Italy

<sup>2</sup> Istituto Fisica Cosmica e Applicazioni all'Informatica (IFCAI), C.N.R., via La Malfa 153, I-90146 Palermo, Italy

<sup>3</sup> Istituto di Astrofisica Spaziale (IAS), C.N.R., via Enrico Fermi 21, I-00044 Frascati, Italy

<sup>4</sup> Dipartimento di Fisica, Università di Ferrara, via Paradiso 12, I-44100 Ferrara, Italy

<sup>5</sup> Astrophysics Division, Space Science Department of ESA, ESTEC, Keplerlaan 1, 2200 AG Noordwijk, The Netherlands

Received 18 September 1997 / Accepted 7 October 1997

**Abstract.** The X-ray pulsar Her X-1 was observed for more than two orbital cycles near the maximum of the 35 day X-ray intensity cycle by the Narrow Field Instruments on-board the *BeppoSAX* satellite. We present the first simultaneous measurement of the 0.1-200 keV spectrum. Three distinct continuum components are evident in the phase averaged spectrum: a low energy excess, modeled as a 0.1 keV blackbody; a power-law and a high energy cut-off. Superposed on this continuum are Fe L and K emission features at 1.0 and 6.5 keV, respectively, and a  $\sim 40$  keV cyclotron absorption feature. The cyclotron feature can be clearly seen in raw count spectra. We present the properties of the cyclotron feature with unprecedented precision and discuss the indications given by this measurement on the physical properties of the emitting region.

**Key words:** X-rays: binaries – individual: Her X-1 – X-rays: cyclotron

## 1. Introduction

Her X-1 is an eclipsing binary X-ray pulsar with an orbital period of 1.7 days and a pulsation period of 1.2 s (Tananbaum et al. 1972; Giacconi et al. 1973). It exhibits a 35 day cycle in X-ray intensity consisting of a  $\sim 10$  day duration main on-state and a shorter duration, a factor  $\sim 3$  fainter, secondary on-state (e.g., Gorecki et al. 1982). This modulation may result from obscuration caused by a precessing tilted accretion disk that periodically obscures the line of sight to the neutron star (e.g.

Katz 1973; Petterson 1975, 1977). In between on-states, Her X-1 is still visible at a low X-ray intensity level (Jones & Forman 1976). A regular pattern of X-ray intensity dips are observed at certain orbital phases during the on-states (Crosa & Boynton 1980; Reynolds & Parmar 1995).

The broad band X-ray spectrum of Her X-1 is known to be complex. In common with other accreting X-ray pulsars, the overall spectral shape in 1-10 keV can be described by a power-law. In the energy range 0.1-200 keV the following additional components have been reported: low-energy absorption consistent with the interstellar value; a  $\sim 100$  eV blackbody which dominates the spectrum below  $\sim 1$  keV (McCray et al. 1982; Oosterbroek et al. 1997); a broad Fe L emission feature at  $\sim 1$  keV (Mihara & Soong 1994; Oosterbroek et al. 1997); a broad Fe K emission feature at  $\sim 6.5$  keV which was studied in detail by Choi et al. (1994) using *Ginga* data; an approximately exponential cut-off to the power-law  $> 10$  keV and a broad feature, centered around 40 keV, which is usually interpreted as a cyclotron absorption or emission feature (Trümper et al. 1978; Voges et al. 1982; Soong et al. 1990; Mihara et al. 1990). Her X-1 was the first cosmic X-ray source from which a cyclotron feature was detected (Trümper et al. 1978).

In this *Letter* we present the first simultaneous measurement of the Her X-1 spectrum over the 0.1-200 keV energy range. The Narrow Field Instruments (NFI) on-board *BeppoSAX* (Boella et al. 1997a) consist of the imaging Low-Energy Concentrator Spectrometer (LECS; 0.1-10 keV; Parmar et al. 1997), the imaging Medium-Energy Concentrator Spectrometer (MECS; 1.5-10 keV; Boella et al. 1997b), the High Pressure Gas Scintillation Proportional Counter (HPGSPC; 3-150 keV; Manzo et al. 1997) and the Phoswich Detector System (PDS; 15-300 keV; Frontera et al. 1997).

Send offprint requests to: D. Dal Fiume  
(e-mail: daniele@tesre.bo.cnr.it)

## 2. Observation

*BeppoSAX* observed Her X-1 between 1996 July 24 00:34 UT and July 27 11:54 UT. Source spectra were extracted excluding intervals when Her X-1 was in eclipse or undergoing X-ray intensity dips. The total source exposure times are 36 ks for the LECS, 90 ks for the MECS, 26 ks for the HPGSPC, and 47 ks for the PDS. The different exposure times are due to rocking collimators (HPGSPC and PDS), to operative time only during satellite night time (LECS) and to different filtering criteria during passages in the South Atlantic Geomagnetic Anomaly and before and after Earth occultations.

Standard data extraction techniques were used for all instruments. That used for the LECS is described in Oosterbroek et al. (1997). In LECS and MECS Her X-1 is a factor  $> 100$  times the background counting rate and so systematic effects in the background subtraction are negligible. The methods of background subtraction using the rocking collimator technique for the HPGSPC and PDS are described in Frontera et al. (1997) and Manzo et al. (1997). The standard collimator rocking angles of  $210'$  for the PDS and  $180'$  for the HPGSPC were used together with a dwell time for each on- and off-source position of 96 s. The systematic error in PDS background subtraction is negligible for sources whose flux is higher than 1 mCrab, including Her X-1 (Guainazzi & Matteuzzi 1997).

### 2.1. The X-ray spectrum

The phase averaged X-ray spectrum was modeled using seven previously observed components: (1) a low-energy excess described by a blackbody of temperature  $kT_{\text{BB}}$ , (2) a Gaussian feature with energy  $E_{\text{L}}$  keV, and full width half-maximum (FWHM) of  $\text{FWHM}_{\text{L}}$  keV, (3) low-energy absorption,  $N_{\text{H}}$ , using the coefficients of Morrison & McCammon (1983) together with the elemental abundances of Anders & Ebihara (1982), (4) a broken power-law continuum with photon indices  $\alpha_1$  and  $\alpha_2$  and break energy  $E_{\text{break}}$ , (5) an Fe K emission feature, (6) a high energy cut-off to the broken power-law and (7) a cyclotron feature. Among these components, the shapes of the high energy cut-off and cyclotron feature are most uncertain. Version 9.0 of the XSPEC spectral fitting program (Arnaud 1996) was used. A total of 15-19 parameters (depending on how the above components were modeled) were allowed to vary during the fits. In addition, the normalization of each of the NFI was allowed to vary in order to help account for the known calibration uncertainties between the instruments. In Table 1 we report the result of the spectral fits using the above seven components and a multiplicative Gaussian (Model 1 – Soong et al. 1990) or a Lorentzian (Model 2 – Mihara et al. 1990) absorption line to model component 7. Unsatisfactory fits were obtained using an emission line.

Given the number of spectral components observed from Her X-1 in different energy ranges by different missions, we expected that a single fit to the entire 0.1-200 keV spectrum would be problematic. For the high energy cut-off and cyclotron feature we tried many of the currently used empirical or semi-

**Table 1.** Spectral fit parameters

Parameter	Model 1	Model 2
$I_{\text{pow}} (\times 10^{-1} \text{ photons cm}^{-2} \text{ s}^{-1})$	$1.083 \pm 0.006$	$1.081 \pm 0.006$
$\alpha_1$	$0.884 \pm 0.003$	$0.882 \pm 0.003$
$\alpha_2$	$1.83 \pm_{0.07}^{0.05}$	$1.77 \pm 0.07$
$E_{\text{break}} \text{ (keV)}$	$17.74 \pm_{0.30}^{0.26}$	$17.86 \pm_{0.32}^{0.21}$
$I_{\text{BB}} (L_{36}/d_{10}^2)$	$0.66 \pm 0.02$	$0.66 \pm 0.02$
$kT_{\text{BB}} \text{ (keV)}$	$0.092 \pm 0.002$	$0.092 \pm 0.002$
$N_{\text{H}} (\times 10^{19} \text{ atoms cm}^{-2})$	$5.1 \pm 0.7$	$5.1 \pm 0.7$
$I_{\text{L}} (\times 10^{-2} \text{ photons cm}^{-2} \text{ s}^{-1})$	$3.53 \pm 0.24$	$3.54 \pm 0.24$
$E_{\text{L}} \text{ (keV)}$	$0.945 \pm 0.012$	$0.945 \pm 0.012$
$\text{FWHM}_{\text{L}} \text{ (keV)}$	$0.390 \pm 0.024$	$0.390 \pm 0.024$
$I_{\text{K}} (\times 10^{-3} \text{ photons cm}^{-2} \text{ s}^{-1})$	$4.88 \pm 0.18$	$4.84 \pm_{0.16}^{0.19}$
$E_{\text{K}} \text{ (keV)}$	$6.55 \pm 0.015$	$6.55 \pm 0.015$
$\text{FWHM}_{\text{K}} \text{ (keV)}$	$1.06 \pm 0.06$	$1.06 \pm 0.06$
$E_{\text{cut}} \text{ (keV)}$	$24.2 \pm 0.2$	$24.3 \pm 0.3$
$E_{\text{fold}} \text{ (keV)}$	$14.8 \pm 0.4$	$15.2 \pm 0.4$
$E_{\text{cycl}} \text{ (keV)}$	$42.1 \pm 0.3$	$40.3 \pm 0.2$
$\text{EW}_{\text{cycl}} \text{ (keV)}$	$14.9 \pm_{1.0}^{1.25}$	-
$\text{FWHM}_{\text{cycl}} \text{ (keV)}$	$14.7 \pm 0.9$	$16.3 \pm 1.4$
$\text{Depth}_{\text{cycl}}$	-	$0.73 \pm 0.03$
$\chi^2_{\nu} \text{ (dof)}$	$1.984 \text{ (908)}$	$1.987 \text{ (908)}$

NOTE - Errors correspond to 90% single parameter confidence level

empirical models, but none of them gave acceptable values of  $\chi^2_{\nu}$ . We can exclude the single harmonic cyclotron absorption model of Mihara et al. (1990) without high energy exponential cutoff and the Fermi-Dirac Cut-Off (FDCO) plus cyclotron absorption model (Mihara 1995), as they gave very high values of  $\chi^2_{\nu}$ . We also obtained worse results using a single (not broken) power law. We report in Table 1 only the results from the best two model fits. These are (1) a broken power law plus high energy exponential cut-off together with a Gaussian absorption feature and (2) a broken power-law plus a high energy exponential cut-off together with a Lorentzian absorption feature (Mihara et al. 1990). The two models give comparable results in term of  $\chi^2_{\nu}$ . While the fit results are still not formally acceptable, given the known systematic uncertainties in the NFI of  $\sim 5\%$ , we do not think it worthwhile adding extra components. The total observed flux at earth in the 0.1-200 keV energy band is  $7.2 \times 10^{-9} \text{ erg cm}^2 \text{ s}^{-1}$  that corresponds to a total observed luminosity of Her X-1  $L_{\text{x}} = 2.15 \times 10^{37} \text{ erg s}^{-1}$ , assuming a distance of 5 kpc.

The broad band spectrum of Her X-1 appears to be even more complex than expected. In particular, the high energy cut-off cannot be modeled satisfactorily using a single power law, neither adding the “classical” exponential cutoff (White et al. 1983), nor adding the more recent cyclotron absorption model of Mihara et al. (1990). This can be clearly seen in the 10-20 keV residuals where large structured variations are present using these models. The use of a broken power law, with an exponential cutoff near 24 keV greatly improves the fit as can be seen from the fit residuals shown in Fig. 1.

The cyclotron feature is clearly visible in the raw count rate spectra. In Fig. 2 (upper panel), the ratio between the Her X-1

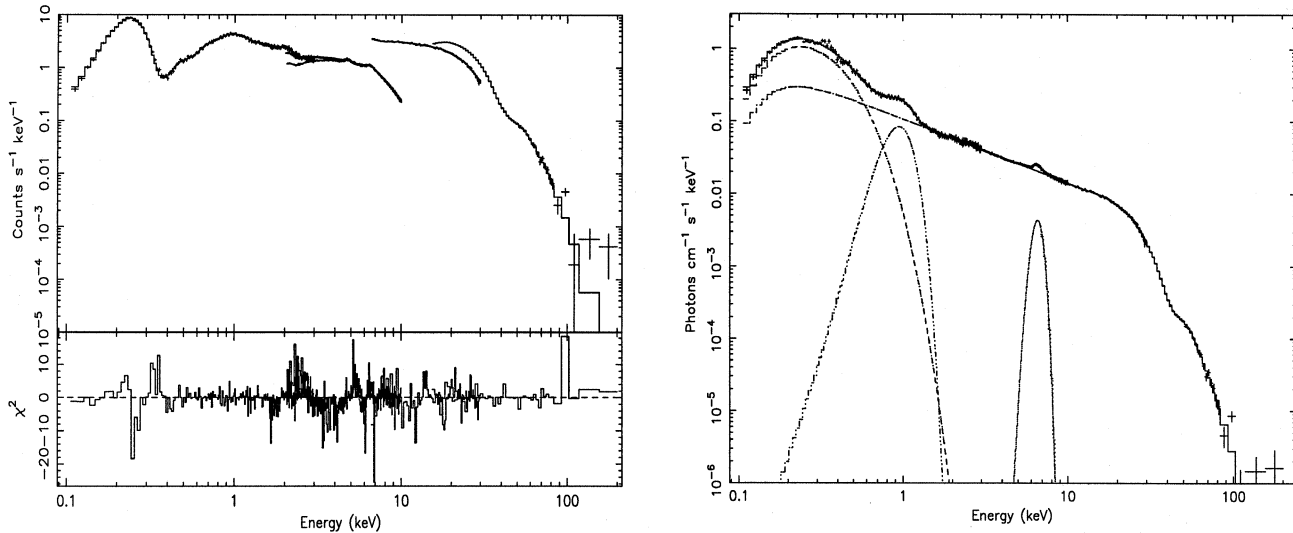


**Fig. 1.** The spectrum of Her X-1 in the 0.1-200 keV energy range observed by the *BeppoSAX* NFI. Left panel: count rate spectrum and contribution to  $\chi^2$ . The best-fit obtained using model 1 is shown as a histogram. Right panel: deconvoluted photon spectrum. The different spectral components used in the fit are indicated by the dashed lines.

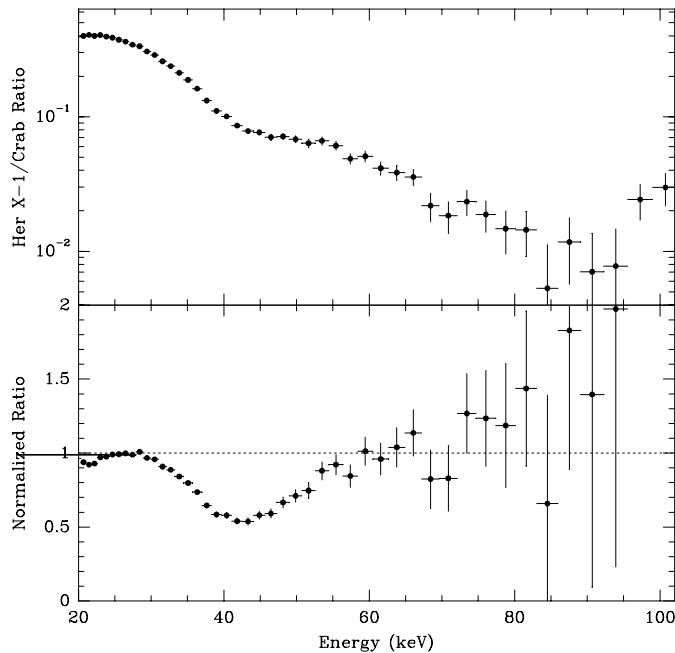


**Fig. 2.** Upper panel: ratio of the 20-100 keV PDS count rate spectra of Her X-1 and the Crab Nebula. Lower panel: the same ratio normalized to the Her X-1 continuum (see text).

and the Crab Nebula count spectra is shown (the Crab Nebula spectrum is expected to be featureless in this energy band). The overall shape of this ratio is dominated by the difference in the shape of the two continua, Her X-1 being harder below  $\sim 23$  keV. A clear deviation from the smooth ratio of the two continua is seen as a broad hump that extends from 40 to 100 keV. This does not have the shape of a narrow emission or absorption line, as expected from previous measurements. Given that the ratio of the spectra is largely independent of the

uncertainties in the energy calibrations and spectral reconstruction, it can be also used to derive a model and calibration-free estimate of the energy at which the Her X-1 spectral shape begins to deviate from the continuum.

In order to more clearly see the shape of the high energy absorption feature, the count rate ratios were multiplied by the slope of the Crab Nebula photon spectrum ( $E^{-2.1}$ ). Then we divided by the continuum functional, namely the broken power law plus high-energy cutoff, which approximates the Her X-1 high energy continuum *without* the cyclotron feature. The effect of these two steps is to obtain a normalized spectrum that approximates the actual photon spectrum, as the division by the Crab Nebula spectrum removes, to first order, the instrumental effects. The effect of the second step is to enhance the deviations of this normalized spectrum from the continuum shape described by the best-fit model. In the continuum functional we used the parameters obtained from the XSPEC fit, model 1 (see Table 1). We obtained an identical result using the continuum functional of model 2. The lower panel of Fig. 2 shows a broad, symmetric absorption line, centered just above 40 keV. As expected, this is in good agreement with the fit parameters listed in Table 1. The count ratio returns consistent with unity above  $\sim 55$  keV. For a cyclotron line energy of 42 keV the magnetic field strength is  $3.5 \times 10^{12}$  G.

### 3. Discussion

The low-energy ( $E < 2$  keV) part of the spectrum is discussed in Oosterbroek et al. (1997) and will not be discussed further here. The Fe K line measurement confirms the findings of Choi et al. (1994). We measure a similar line energy and width. Our spectral resolution, while a factor  $\sim 3$  better than that of *Ginga* LAC, does not allow the structure of the line to be further investigated. A slightly asymmetric shape supports the hypothesis of Choi

et al. that the feature is a blend originating from multiple lines at different degrees of ionization.

The underlying shape of the continuum of X-ray pulsars is still an open question. Following the first studies of scattering and opacities in strongly magnetized plasmas (e.g. Canuto et al. 1971) various attempts to predict the shape of the emitted X-ray spectrum have been made. Monte-Carlo methods were used by Mészáros & Nagel (1985a, 1985b, hereafter MN-I and MN-II) to calculate spectra, cyclotron line shapes and pulse profiles. They use a magnetic field intensity of  $3.3 \times 10^{12}$  G, which gives a cyclotron energy of 38 keV. This choice is close to our measured value in the case of Her X-1, and therefore their results can be readily compared to our spectrum. Our measurement strongly indicates that the cyclotron feature is in absorption, in agreement with the model calculations. The model predicts a line FWHM ( $\Delta\omega_B$ ), dependent on the angle between the line of sight and the field direction,  $\theta$ , broader for smaller angles. Using Eq. 13 in MN-I,

$$\Delta\omega_B \simeq \omega_B \left( 8 \times \ln(2) \times \frac{kT_e}{m_e c^2} \right)^{\frac{1}{2}} |\cos \theta| \quad (1)$$

where  $\omega_B$  is the cyclotron line frequency, and  $m_e c^2$  is the electron rest mass, and assuming  $|\cos \theta| \approx 1$ , we obtain a lower limit of the electron temperature  $kT_e$  of approximately 11 keV (we used a line width of  $\sim 15$  keV – see Table 1). This is in fair agreement with the calculations of self-emitting atmospheres of Harding et al. (1984). In the case of a magnetic field of  $3.5 \times 10^{12}$  G the predicted temperature for a slab or column with optical depth of the order of  $50 \text{ g cm}^{-2}$  (Mészáros et al. 1983) is approximately  $4\text{--}8 \times 10^7$  °K, which corresponds to  $kT_e \sim 3.5\text{--}7$  keV. Harding et al. (1984) predict higher temperatures for higher magnetic fields. This is also in agreement with *BeppoSAX* observations of Her X-1 and Vela X-1 (Orlandini et al. 1997). Indeed, in the case of Vela X-1 the cyclotron energy is 60 keV and the FWHM is  $\sim 26$  keV, corresponding to an electron temperature of approximately 18 keV. The harder spectrum observed from Vela X-1 also confirms the correlation between spectral hardness and magnetic field intensity (see also Frontera & Dal Fiume 1989; Makishima et al. 1990). The low energy power-law is reproduced in MN-I and MN-II qualitatively, and has a spectral photon index somewhat flatter than our observed value of  $\sim -0.8$ .

More recent models on line profile and widths (Araya and Harding, 1996) were obtained for A0535+26, using a magnetic field intensity much higher than that measured in Her X-1. No analytical model neither for the spectrum nor for the line profile is available, therefore their results cannot be compared with our measurement. They caution that the “classical” estimate of electron temperature using line width, as in Eq. 1, can be flawed and suggest an estimate taken from Lamb et al. (1990)

$$T_e = \frac{\omega_B}{(2 + \alpha_{\text{eff}})} \quad (2)$$

that is valid in the limit of a single scattering. In this relation  $\alpha_{\text{eff}}$  is the effective power law slope at the cyclotron line. The

spectrum of Her X-1 cannot be approximated above 20 keV with a power-law, but a rough estimate of the slope gives values of 3.5-5. Assuming the centroid of the cyclotron feature at 42 keV we obtain, from Eq. 2, an estimate of the electron temperature  $T_e$  of 6-7.6 keV.

The empirical models used here to fit the broad band spectrum of Her X-1 are clearly inadequate to extract all the information about the physical properties of the emitting region. However this work illustrates the importance of broad band studies of X-ray pulsars in gaining insight into the physical processes of the emission region. In particular, better analytical models of both continuum and lines can give better and more reliable estimates of the physical properties of the emitting region as electron temperature, density and size of the emitting region.

*Acknowledgements.* We thank the *BeppoSAX* Science Team, the *BeppoSAX* SDC and the Nuova Telespazio staff at the *BeppoSAX* Control Center for their support. This research was in part supported by a dedicated grant of Agenzia Spaziale Italiana.

## References

- Anders, E., Ebihara, M. 1982, *Geochim. Cosmochim. Acta*, 46, 2363  
 Araya, R.A., Harding, A.K. 1996, *ApJ*, 463, L33  
 Arnaud, K.A., 1996, In: Jacoby G., Barnes J. (eds.) *Astronomical Data Analysis Software Systems V*, ASP Conf. Series, 101, p.17  
 Boella, G., Butler, R.C., et al. 1997a, *A&AS*, 122, 299  
 Boella, G., Chiappetti, L., et al. 1997b, *A&AS*, 122, 327  
 Canuto, V., Lodenquai, J., Ruderman, M. 1971 *Phys. Rev.*, D3, 2303  
 Choi, C.S., Nagase, F., Makino, F. 1994, *ApJ*, 437, 449  
 Crosa, L., Boynton, P.E. 1980, *ApJ* 235, 999  
 Frontera, F., Costa E., et al. 1997, *A&AS*, 122, 357  
 Frontera, F., Dal Fiume, D. 1989, In: *Proc. 23<sup>th</sup> ESLAB Symposium*, ESA SP-296, p.37  
 Giacconi, R., Gursky, H., et al. 1973, *ApJ*, 184, 227  
 Gorecki, A., Levine, A., et al. 1982, *ApJ*, 56, 234  
 Guainazzi, M., Matteuzzi, A. 1997, *BSAX-SDC TR-011*  
 Harding, A.K., Mészáros, P., et al. 1984, *ApJ*, 278, 369  
 Jones, C., Forman, W. 1976, *ApJ*, 209, L131  
 Katz, J.I. 1973, *Nature Phys. Sci.*, 246, 87  
 Lamb, D.Q., Wang, J.C.L., Wasserman, I.M. 1990, *ApJ*, 363, 670  
 Makishima, K., Mihara, T., et al. 1990, *ApJ*, 365, L59.  
 Manzo, G., Giarrusso, S., et al. 1997, *A&AS*, 122, 341  
 McCray, R.A., Shull, J.M., et al. 1982, *ApJ*, 262, 301  
 Mészáros, P., Harding, A.K., et al. 1983, *ApJ*, 266, L33  
 Mészáros, P., Nagel, W. 1985a, *ApJ*, 298, 147 (MN-I)  
 Mészáros, P., Nagel, W. 1985b, *ApJ*, 299, 138 (MN-II)  
 Mihara T. 1995, Ph.D. Thesis, Riken.  
 Mihara, T., Makishima, K., et al. 1990, *Nat*, 346, 250  
 Morrison, R., McCammon, D. 1983, *ApJ*, 270, 119  
 Orlandini, M., Dal Fiume, D., et al. 1997, *A&A*, submitted  
 Oosterbroek, T., Parmar, A.N., et al. 1997, *A&A*, in press  
 Parmar, A.N., Martin, D.D.E., et al. 1997, *A&AS*, 122, 309  
 Petterson, J.A., 1975 *ApJ*, 201, L61  
 Petterson, J.A. 1977, *ApJ*, 218, 783  
 Reynolds, A.P., Parmar, A.N. 1995, *A&A*, 297, 747  
 Soong, Y., Gruber, D.E., et al. 1990, *ApJ*, 348, 641  
 Tananbaum, H., Gursky, H., et al. 1972, *ApJ*, 174, L143  
 Trümper, J., Pietsch, W., et al. 1978, *ApJ*, 219, L105  
 Voges, W., Pietsch, W., et al. 1982, *ApJ*, 263, 803  
 White, N.E., Swank, J.H., Holt, S.S. 1983, *ApJ*, 270, 711